Applications of Mathematics

Joseph M. Maubach

Space-filling curves for 2-simplicial meshes created with bisections and reflections

Applications of Mathematics, Vol. 50 (2005), No. 3, 309–321

Persistent URL: http://dml.cz/dmlcz/134608

SPACE-FILLING CURVES FOR 2-SIMPLICIAL MESHES CREATED WITH BISECTIONS AND REFLECTIONS

Joseph M. Maubach, Eindhoven

Abstract. Numerical experiments in J. Maubach: Local bisection refinement and optimal order algebraic multilevel preconditioners, PRISM-97 conference Proceedings, 1977, 121–136 indicated that the refinement with the use of local bisections presented in J. Maubach: Local bisection refinement for n-simplicial grids generated by reflections, SIAM J. Sci. Comput. *16* (1995), 210–227 leads to highly locally refined computational 2-meshes which can be very efficiently load-balanced with the use of a space-filling curve. This paper introduces the construction of this curve which can be produced at almost no costs, proofs that all its properties are invariant under local bisection, and comments on the 3-dimensional case.

With the use of a space-filling curve (which passes through all triangular elements), load balancing over several processors is trivial: The load can be distributed over N processors by cutting the curve into N almost equilength parts. Each processor then operates on the triangles which are passed by its part of the curve.

Keywords: grid generation, space filling curve, load balancing

MSC 2000: 65M50

1. Introduction

Refinement with the use of local bisection has been examined and discussed in [1], [14], [7], [9] and [8], [4], [3], [13] and [12]. The local bisection refinement in [7] is simplest and efficient, and it is suited for modern challenging applications such as optics and on-chip-interconnects (Fig. 1 shows an on-chip resistor).

In all such applications, the domains of interest are a coarse tensor product mesh refined with the use of local bisection. These challenging applications require massive parallel calculations (even massive parallel methods such as in [5], [6]), which at their turn require a load balance algorithm.

This paper complements the local bisection method in [7] with a local curve adaptation method such that, independently of the level of refinement, the curve traverses

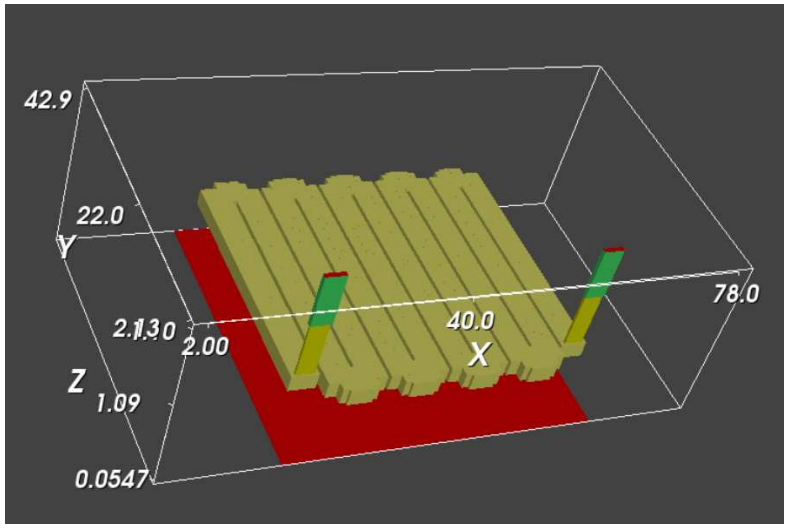

Figure 1. An on-chip resistor.

all 2-simplices once and does not intersect/touch itself (see (P1) and (P2) in Section 2). The fact that one such curve traverses all elements through midpoints of facets without selfintersection is not trivial, because some simple meshes will not permit one curve (see Fig. 2). Furthermore, the manner in which the curve traverses all simplices (possible descendents created by refinement) is special (see (P1)): The amount of vertices at the border of a subdomain will be small: Fast communication.

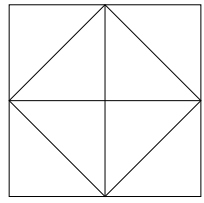

Figure 2. A single non-intersecting curve is not always possible.

The local curve adaptation method uses but the stored n-simplex data (coordinates of the 3 vertices or levels of the 1-facets) and hence comes at negligible costs. The curve adaptation method is defined with the introduced concept of "the level of a 1-facet". The different experimentally determined adaptation method presented in [10] produces identical curves (commented on in Section 2).

The curve can be used to put the elements in curve-traversal order, and the required load-balance redistribution amounts to a possible inexpensive move of some head-part- or tail-part-elements to another processor.

Section 2 presents the bisection method [7], introduces the concept of clusters and facet-levels, defines the curve per element and proves that it remains connected and non-intersects under refinement. Then, Section 3 discusses expectations for the 3-dimensional case, and Section 4 formulates the conclusions.

2. The local curve adaptation method

This section discusses the construction of the curve. First, we introduce the bisection method from [7], and prove that compatible 2-elements always turn out to be also elements of one of a sequence of uniform meshes. The related lines of symmetry are assigned a unique level, and 1-facets inherit the level of the line on which they are situated. Then, the curve per element is defined with the use of these levels. Note that not all meshes permit a spacefilling curve (see Fig. 2), this paper just proves that meshes created with the local bisection method presented in [7] do so.

The local refinement presented in [7] starts from a coarse mesh Ω_1 (see Fig. 5) where elements are all similar under reflection (horizontal and vertical lines) and permutations (skew lines). Then the applied local bisections lead to a refined mesh (see Fig. 4).

Each local bisection involves one or two elements which share the 1-facet to be bisected ([7]). Each of these elements is bisected into 2 descendents (also called its children). As an example, consider Fig. 3. Here one element is bisected multiple times, which leads to four descendents. For each numbered elements, the 1-facet to be bisected is marked with a black bullet. By construction (see [7]) elements 4 and 6 are compatible, but 3 and 4 are not. Fig. 5 shows collections of compatible elements (A–E).

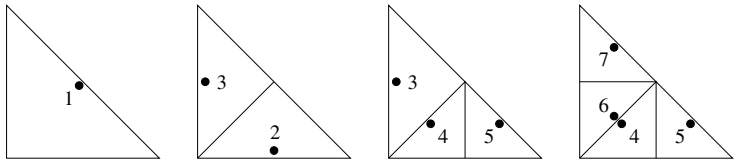

Figure 3. Three subsequent bisection steps.

To start with, we need the following property, which was not proven in [7] because that paper was restricted to the general n-dimensional case.

Lemma. *All 2-elements in a locally refined mesh have their 1-facet to be bisected opposite the $\pi/4$ angle.*

P r o o f. Fig. 3 shows that this holds under bisection (these are all cases in two dimensions, see [7]). The property holds for all four elements of Ω_1 in Fig. 5 (see [7]).

Hence, by induction under refinement, the property holds for all elements in a locally refined mesh. □

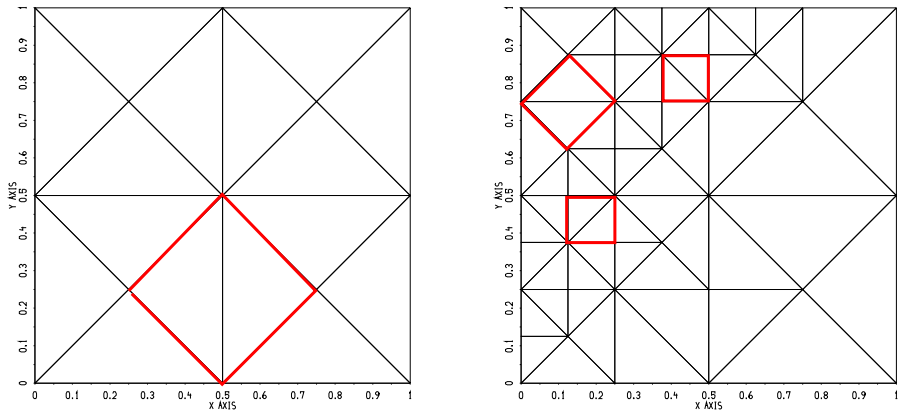

Figure 4. The coarse mesh and the refined mesh.

For the sake of brevity, we use the word *cluster* for *a compatible pair of 2-elements to be bisected*. Note that a cluster in a refined mesh (see Fig. 4) is also a cluster A–D in a uniform mesh (see Fig. 5). The vertices of elements of a uniform mesh are on a lattice (are at regularly spaced positions) whence also the vertices of an element in a cluster are on a lattice. The x and y-coordinates of each lattice are of the form $k/2^L$ for $L > 0$ and $k \in \{0, 1, \ldots, 2^L - 1\}$ and its lines of symmetry are either $y = x$, $y = 1 - x$, $y = 0$ and $x = 0$ or images under a shift of the form $k/2^L$ for $L \geqslant 0$ and $k \in \{0, 1, \ldots, 2^L - 1\}$.

Our construction of a space-filling curve for a cluster of elements in a refined mesh will make use of the horizontal and skew lines in the lattice which contains this cluster, as follows.

Definition. Let $k \bmod 2^L = 1$ or $L = 0$. The levels of each line in the lattice Ω_1, $\Omega_2, \ldots, \Omega_L, \ldots$ in Fig. 5 are:

line	level
$y = x + k/2^L$	level $2L + 1$
$y = 1 - x + k/2^L$	level $2L + 1$
$y = k/2^L$	level $2L + 1$
$x = k/2^L$	level $2L + 1$

Table 1. Lattice line levels.

Note that the highest level line in the lattice Ω_L is L and that the bisection of a cluster in Ω_L creates a new 1-facet on a line of level $L + 1$. An element in Ω_L has

vertices with coordinates of the form

$$\frac{k}{2^{\lceil L/2 \rceil}}, \tag{1}$$

where $\lceil \cdot \rceil$ stands for round upwards to the nearest integer value. Furthermore, observe that each element of Ω_L has at least one horizontal/vertical 1-facet of level L.

Definition. Let the 2-element in a (refined) mesh be an element in one of the uniform meshes Ω_L. Then the level of one of its 1-facets is equal to the level of the line which contains this facet.

Definition. For each 2-element in the (refined) mesh, its curve connects the midpoints of its two highest-level 1-facets.

Based on the level of the edges of Ω_1 (see Fig. 5), the related curve is a multi-line through $(1/4, 1/4)$, $(3/4, 1/4)$, $(3/4, 3/4)$, $(1/4, 3/4)$, which is connected and non-self-intersecting. Left to be proven is that

(P1) subsequently traverses both its children;
(P2) remains connected (does not intersect/touch itself)

and they remain invariant under bisection. In order to show this, we distinguish 5 cases A–E, see Fig. 5. The cases A and B are all different cluster orientations in Ω_L with L even, the cases C and D all cluster orientation in Ω_L with L odd, and the cases E are all cases of clusters from A–D with one or more 1-facets at one of the boundaries.

Lemma. *There are (apart from translation)* 5 *different cluster orientations on each lattice* $\Omega_1, \Omega_2, \ldots$*, called A, B, C and D. Clusters on the boundaries are denoted E.*

Lemma. *The bisection of a cluster of orientation A satisfies* (P1) *and* (P2).

P r o o f. From the coordinates of one of the vertices of the cluster, by and by, we determine all levels of its 1-facets (first three columns of Fig. 6). Based on these levels, we show how the curve traverses the cluster or the bisected cluster (last two columns of Fig. 6).

Note that a cluster of orientation A is on a lattice of the form $\Omega_{2 \cdot L}$. It has a base point (shown in Fig. 5) of the form $(x_b, y_b) = (k/2^L, l/2^L)$, where $\bmod(k - l, 2) = 0$. We will distinguish 2 cases, k even and k odd.

First assume k is even, the case depicted in the first row of Fig. 6. Now, because k is even and $\bmod(k - l, 2) = 0$, also l is even. This yields the first two levels of the

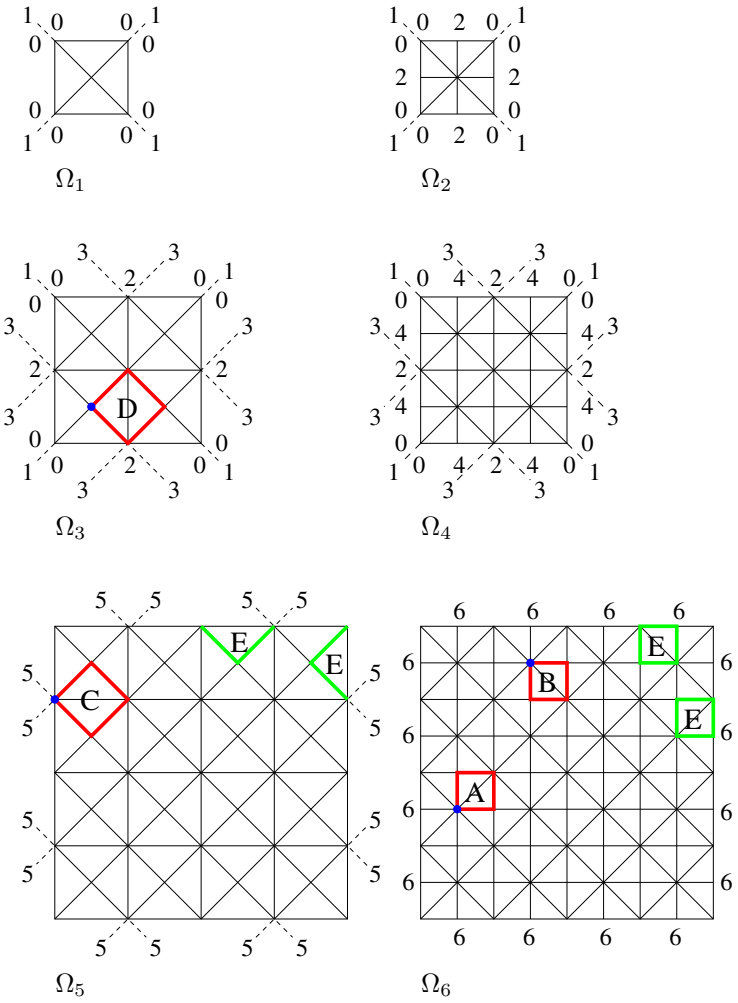

Figure 5. The sequence of uniform refined meshes (lattices).

1-facet, shown in the first column of Fig. 6 (recall that one of the horizontal and one of the vertical lines are of level $2L$).

Now assume $x \geqslant y$ (the other case $y \geqslant x$ can be treated indentically). Then we know that there exist $K > 0$, $N \geqslant 0$ and odd numbers x_{odd} and y_{odd} such that we can factor:

$$x_b = \frac{2^K \cdot 2^N \cdot x_{\text{odd}}}{2^L}, \quad y_b = \frac{2^K \cdot y_{\text{odd}}}{2^L}. \tag{2}$$

First assume that $N > 0$ (k still even). Then from

$$x_b = \frac{x_{\text{odd}}}{2^{L-K-N}}, \quad y_b = \frac{y_{\text{odd}}}{2^{L-K}} \tag{3}$$

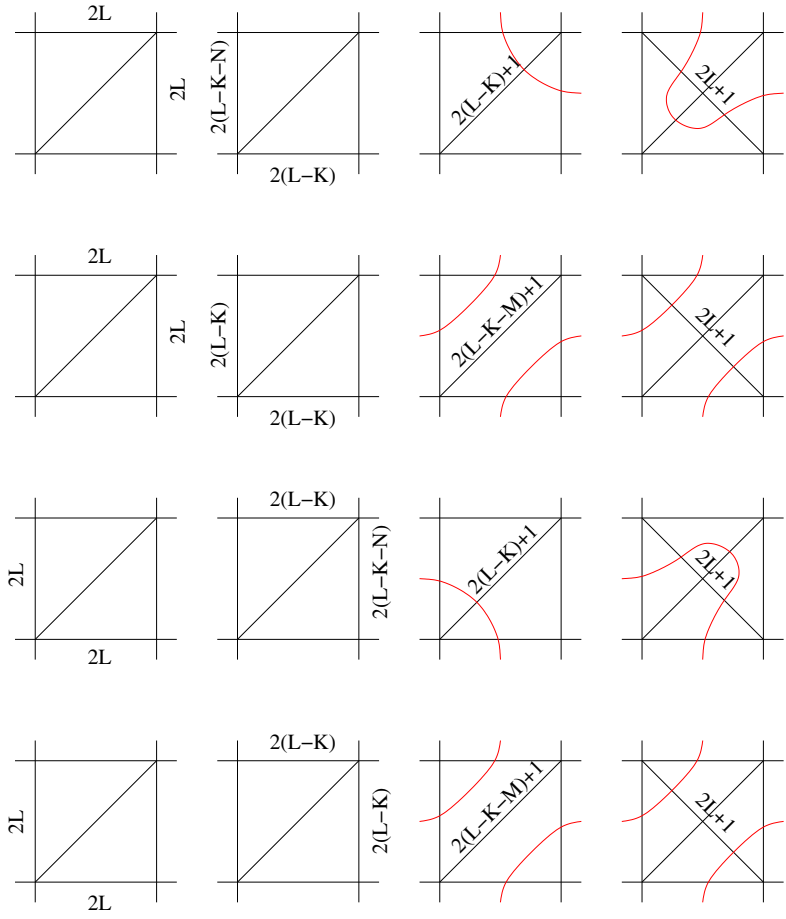

Figure 6. Orientations A: Local bisection keeps the curve connected.

we obtain the level of the other two horizonal/vertical 1-facets (the 2nd column of the first row in Fig. 6). For the level of diagonals, observe that the diagonal is a line of the form

$$y = x + y_b - x_b, \tag{4}$$

where the difference $y_b - x_b$ determines the level:

$$y_b - x_b = \frac{2^K 2^N x_{\text{odd}}}{2^L} - \frac{2^K y_{\text{odd}}}{2^L} = \frac{2^N x_{\text{odd}}}{2^{L-K}} - \frac{y_{\text{odd}}}{2^{L-K}} = \frac{z_{\text{odd}}}{2^{L-K}}, \tag{5}$$

where z_{odd} is odd (the difference between an even and an odd number), which (see the table with lattice line levels) implies that our diagonal's level is $2(L-K)+1$, depicted in the 3rd column of the first row in Fig. 6. Because the 1-facet created

in the bisection step will be of level $2L+1$ we can depict the form of the curve in the last 2 columns of the first row of Fig. 6. This shows that the curve subsequently traverses both children, and that it remains connected under the bisection step. This concludes case (2) for $N > 0$.

Now assume that $N = 0$ (k still even). This determines the levels of the other two horizonal/vertical 1-facets (the 2nd column of the second row in Fig. 6 (where now $N = 0$). The level of the diagonal can be determined from

$$y_b - x_b = \frac{2^K x_{\text{odd}}}{2^L} - \frac{2^K y_{\text{odd}}}{2^L} = \frac{x_{\text{odd}}}{2^{L-K}} - \frac{y_{\text{odd}}}{2^{L-K}} = \frac{2^M z_{\text{odd}} d}{2^{L-K}} = \frac{z_{\text{odd}} d}{2^{L-K-M}} \tag{6}$$

where z_{odd} is an odd number and $M > 0$. Hence, here the level of the diagonal is $2(L-K-M)+1$ (the 3rd column of the second row in Fig. 6) and (P1) and (P2) hold for the related curves in the last two columns of Fig. 6.

To conclude with, consider the case when k is odd. Also here assume that $x_b \geqslant y_b$. This proof follows in the same manner. The first two levels (the 1st column of the 3rd and 4th rows in Fig. 6) are known because

$$x_b = \frac{x_{\text{odd}}}{2^L}, \quad y_b = \frac{y_{\text{odd}}}{2^L}. \tag{7}$$

The other two horizontal/vertical lines' and the diagonal's levels follow best from the top right vertex of the cluster,

$$(x'_b, y'_b) = \left(\frac{1 + x_{\text{odd}}}{2^L}, \frac{1 + y_{\text{odd}}}{2^L} \right),$$

where $1 + x_{\text{odd}}$ and $1 + y_{\text{odd}}$ are even. Now we follow the line of the proof of the k even case: It follows that there exist $K > 0$, $N \geqslant 0$ and odd numbers x_{odd} and y_{odd} such that we can factor:

$$x'_b = \frac{2^K \cdot 2^N \cdot x_{\text{odd}}}{2^L}, \quad y'_b = \frac{2^K \cdot y_{\text{odd}}}{2^L}, \tag{8}$$

which determines the two levels shown in the 2nd column of the last two rows in Fig. 6. For the level of the diagonal, observe that for $N > 0$ we have

$$y'_b - x'_b = \frac{2^K 2^N x_{\text{odd}}}{2^L} - \frac{2^K y_{\text{odd}}}{2^L} = \frac{2^N x_{\text{odd}}}{2^{L-K}} - \frac{y_{\text{odd}}}{2^{L-K}} = \frac{z_{\text{odd}} d}{2^{L-K}}, \tag{9}$$

and for $N = 0$

$$y'_b - x'_b = \frac{2^K x_{\text{odd}}}{2^L} - \frac{2^K y_{\text{odd}}}{2^L} = \frac{x_{\text{odd}}}{2^{L-K}} - \frac{y_{\text{odd}}}{2^{L-K}} = \frac{2^M z_{\text{odd}} d}{2^{L-K}} = \frac{z_{\text{odd}} d}{2^{L-K-M}}, \tag{10}$$

which leads to the 3rd column of the 3rd or 4th row, respectively, in Fig. 6. □

N o t e. The proof that the curve possesses all properties for the cluster orientation in case A relies on the fact that all levels of all 1-facets can be calculated from one of the cluster's vertices $(x_b, y_b) = (k/2^L, l/2^L)$. The amount of factors 2 in k determines the level of the vertical 1-facets, that amount in l determines the level of the horizontal 1-facets, and that in $k - l$ the level of the diagonal.

Lemma. *The bisection of a cluster of orientation* B–E *satisfies* (P1/2).

P r o o f. Also here, all levels can be calculated from the amount of factors 2 in k and l. For case B, use vertex $(x_b, y_b) = (k/2^L, l/2^L)$ shown in Fig. 5 and proceed as in case A (also distinguish k odd and even). Also here either k and l have the same amount of factors 2 (row 2 Fig. 7) whence $l - k$ has extra factors 2 ($M > 0$), or k and l have a different amount of factors of 2 (row 2 Fig. 7) ($N > 0$) whence $l - k$ has no extra factors of 2.

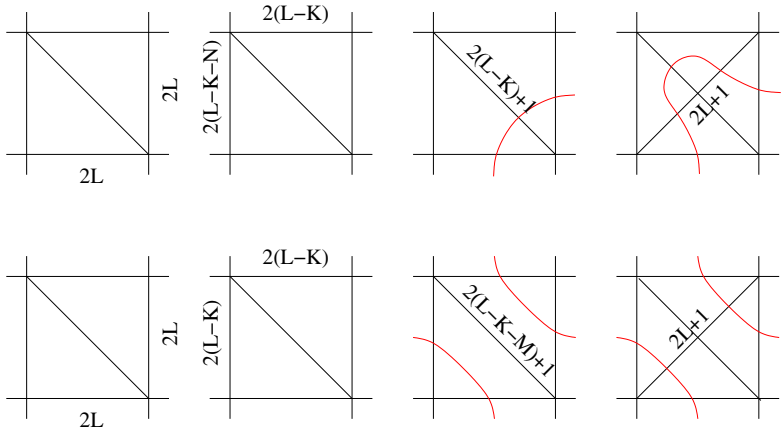

Figure 7. Orientations B: Local bisection keeps the curve connected.

Case C: Here $(x_b, y_b) = (k/2^L, l/2^L)$ is such that k and l are both even or both odd. Two of the diagonals must be of level $2(L-1)+1$. Also here the count of factors 2 leads to the desired results: If k and l have an identical amount of factors 2 then $k - l$ and $k + l + 2^L$ have extra factors 2, which explains the fact that $M > 0$ and $N > 0$ in columns 2 and 3 of row 1 of Fig. 8. The other case when k and l have different amounts of factor 2 needs more attention: Either $K = 1$ (which is the minimum) and we end up in the 2nd row of Fig. 8, or $K > 1$ and we end up in the 1st row of this figure. Case D can be treated in a manner identical to case C.

Cases E can be treated as A–D with the difference that the boundary lines have level 0 and that we know that either k or l is of the form 2^L or 0, which has the desired impact on the amount of factors of 2. □

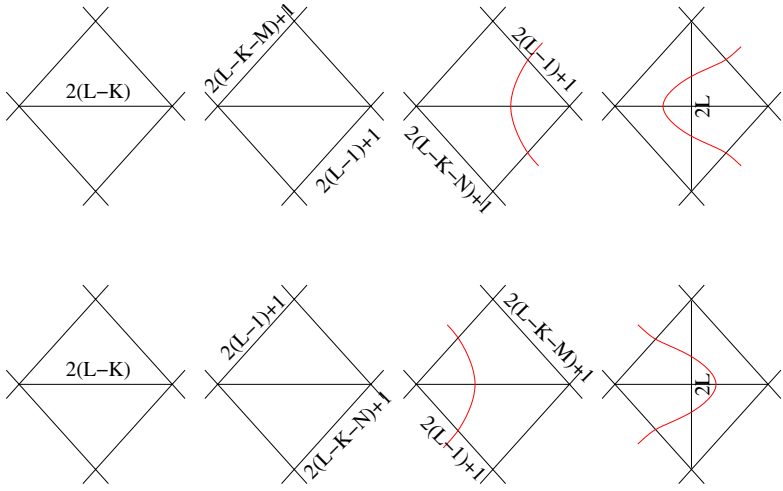

Figure 8. Orientations C: Local bisection keeps the curve connected.

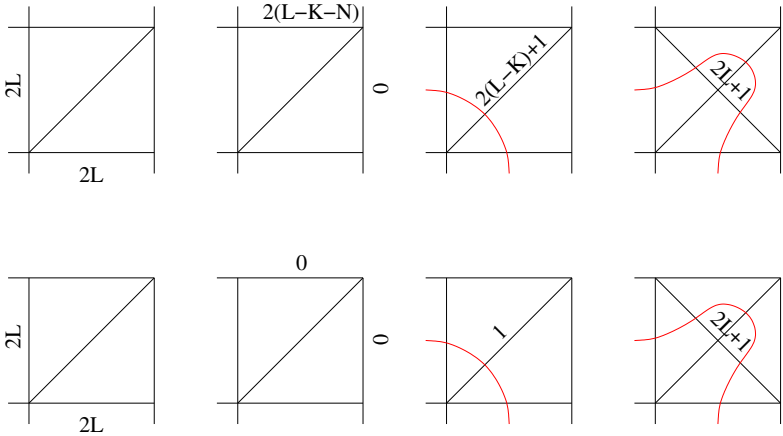

Figure 9. Orientations E: Local bisection keeps the curve connected.

R e m a r k . Note that (P1) mentions "*subsequently traverses both children*". This implies that once a curve enters an element through its facet, it will not leave this element until all its subsequently created descendents have been traversed, which is what makes the communication between processors "minimal" (see Fig. 10 where the space-filling curve of elements is cut into four approximately equi-length pieces).

The experimentally determined spacefilling curve in [10] turns out to be identical (under the same order of refinements applied to the same initial mesh) with the curve shown in Fig. 10. This is remarkable because in [10] a different strategy is followed: First, observe that the space-filling curve enters and exits each individual

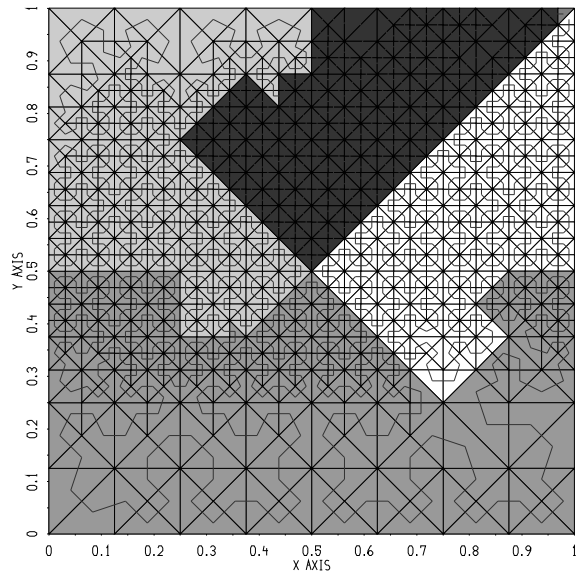

Figure 10. The load-balance result.

triangle. Assume that a triangle is refined and that the curve will now pass through its two descendents. Then the only choice is to determine through which descendent it passes first. To determine which is first, [10] uses the orientation of the parent element. More precisely, let the parent element's vertices be $\mathbf{v}_0$, $\mathbf{v}_1$ and $\mathbf{v}_2$, and let $A = [\mathbf{v}_1 - \mathbf{v}_0 | \mathbf{v}_2 - \mathbf{v}_0] \in \mathbb{R}^{2\times 2}$ be defined column-wise. Then [10] applies an in-situ Householder QR transformation to A (see [2], p. 196) and uses the sign of the product of the diagonal elements—which determines the orientation—to determine which of the children is first. Note that [10] contains no proof that its descendent-based strategy leads to a space-filling curve, just numerical corroboration.

3. Extensions and tetrahedral meshes

The proof that the curve fulfils (P1) and (P2) remains valid if the coarse mesh is obtained under an invertable map F from the standard coarse mesh in $[0,1]^2$. In this case one can extract the level information from the coordinates $F^{-1}(x)$ instead of from the coordinates x. For more information on possible extensions, see [7].

Also in the 3-dimensional case, compatible clusters are forecasted to be clusters in a uniform mesh (the uniform mesh where all elements have the same level as the elements in the cluster, see [7]). However, the determination of the amount of similar cluster orientations is not trivial. This, and whether our 2-factor-amount approach will still work for the extra symmetry lines, is currently under examination.

4. Conclusions

The local bisection refinement method from [7] can be complemented with a local adaptation method which determines a curve for load balance purposes in the 2-d case. Both the local refinement and the curve adaptation method are simple to formulate, simple to implement, and execute very efficiently. With the curve, the load-balancing is simple and the communication of which processor is to process which elements after refinements is fast: Each processor has a chain of elements to process and after a sequence of refinements, it receives or deletes elements to be processed at the start and/or end of its chain.

References

[1] *E. Bänsch*: Local mesh refinement in 2 and 3 dimensions. IMPACT Comput. Sci. Eng. *3* (1991), 181–191.

[2] *G. H. Golub, C. F. Van Loan*: Matrix Computations, 2nd edition. The Johns Hopkins University Press, Baltimore, 1989.

[3] *B. Joe, A. Liu*: On the shape of tetrahedra from bisection. Math. Comput. *63* (1994), 141–154.

[4] *I. Kossaczky*: A recursive approach to local mesh refinement in two and three dimensions. J. Comput. App. Math. *55* (1994), 275–288.

[5] *W. J. Layton, J. M. Maubach, and P. J. Rabier*: Robustness of an elementwise parallel finite element method for convection-diffusion problems. SIAM J. Sci. Comput. *19* (1998), 1870–1891.

[6] *W. Layton, J. M. Maubach, and P. Rabier*: Parallel algorithms for maximal monotone operators of local type. Numer. Math. *71* (1995), 29–58.

[7] *J. Maubach*: Local bisection refinement for n-simplicial grids generated by reflections. SIAM J. Sci. Comput. *16* (1995), 210–227.

[8] *J. Maubach*: The efficient location of simplicial neighbors for locally refined n-simplicial grids. In: Proceedings of the 5th International Meshing Roundtable, Pittsburgh, October 1996. 1996, pp. 137–153.

[9] *J. Maubach*: Iterative Methods for Non-Linear Partial Differential Equations. CWI, Amsterdam, 1994.

[10] *J. Maubach*: Local bisection refinement and optimal order algebraic multilevel preconditioners. In: PRISM-97 conference Proceedings (O. Axelsson et al., eds.). University of Nijmegen, 1997, pp. 121–136.

[11] *W. F. Mitchell*: Optimal multilevel iterative methods for adaptive grids. SIAM J. Sci. Stat. Comput. *13* (1992), 146–167.

[12] *A. Mukherjee*: An adaptive finite element code for elliptic boundary value problems in three dimensions with applications in numerical relativity. PhD. Thesis. Penn State University, 1996.

[13] *A. Plaza, J. P. Suárez, M. A. Padrón, S. Falcón, and D. Amieiro*: Mesh quality improvement and other properties in the four-triangles longest-edge partition. Comput. Aided Geom. Des. *21* (2004), 353–369.

[14] *M. C. Rivara, C. Levin*: A 3-D refinement algorithm suitable for adaptive and multi-grid techniques. Commun. Appl. Numer. Methods *8* (1992), 281–290.

Author's address: *J. M. Maubach*, Department of Mathematics, Eindhoven University of Technology, Eindhoven, The Netherlands, e-mail: `j.m.l.maubach@tue.nl`.